



## Chapter 12

# Evaluating the Coefficient of Thermal Expansion of Electronic Board Using the Virtual Fields Method

Yohei Kanai, Shuichi Arikawa, Satoru Yoneyama, and Yasuhisa Fujimoto

**Abstract** This paper proposes a method for identifying the coefficient of thermal expansion of dissimilar materials. Dissimilar materials are simulating on an electronic packaging. Displacement data used for inverse analysis are obtained by digital image correlation which is a method for measuring displacement in the full field of view without contact. The virtual fields method based on the principle of virtual work is employed as a method for inverse analysis. Each coefficient of thermal expansion that is unknown parameters is determined by preparing virtual displacements as many as the number of unknowns. The effectiveness of the inverse analysis method is demonstrated by identifying the coefficients of thermal expansion of dissimilar materials. Results show that the coefficient of thermal expansion can be obtained by the proposed method.

**Keywords** Coefficient of thermal expansion · Inverse analysis · Virtual fields method · DIC · Electronic board

## Introduction

Electronic circuit boards are a mechanical component of electronics used in railway vehicles, automobiles, elevator control devices, etc. They are made of various materials such as metal, resin and ceramics having different mechanical properties. A difference in the coefficient of thermal expansion of the materials can lead to large thermal stress and strain from heat generation in device and changes in ambient temperature, leading to device failure. Therefore, repeated thermal stress and strain occur on the mounting board due to repeated application of heat on elements and parts on the board due to turning on and off of the electronic equipment under harsh environments of high voltage and large current [1]. Due to this repeated thermal stress, peeling and cracking are caused in solder of parts and bonded parts such as resin, which is considered as one of causes of failure. For designing various products and structures, it is important to understand the material characteristics constituting those devices and structures. In recent years, along with high performance, compactness, weight reduction, and cost reduction of electronic devices and products, the miniaturization and the densification of mounting boards are progressing. Material properties in device may be different from the values obtained from the conventional tensile tests with bulk specimens. Therefore it is necessary to accurately ascertain the coefficient of thermal expansion of the minute parts and structures contained in electric substrate.

As a method for identifying the material properties, it is effective to apply a load to the actual equipment structure and perform inverse problem analysis with the measurement results of displacement and strain obtained as input data. The Virtual Fields Method (VFM) proposed by Grediac et al. [2] is based on the principle of virtual work. It is a method for identifying material properties in a constitutive equation, and the research has been actively conducted in recent years [3, 4]. As a past study, Sato et al. [5] identified elastic material characteristic distribution of dissimilar materials using VFM. This method is effective for identifying material properties of heterogeneous materials.

---

Y. Kanai (✉) · S. Yoneyama

Department of Mechanical Engineering, Aoyama Gakuin University, Sagami-hara-shi, Kanagawa, Japan  
e-mail: [c5618132@aoyama.jp](mailto:c5618132@aoyama.jp); [yoneyama@me.aoyama.ac.jp](mailto:yoneyama@me.aoyama.ac.jp)

S. Arikawa

Department of Mechanical Engineering Informatics, Meiji University, Tama-ku, Kawasaki-shi, Kanagawa, Japan  
e-mail: [arikawa@meiji.ac.jp](mailto:arikawa@meiji.ac.jp)

Y. Fujimoto

Mitsubishi Electric Corporation Advanced Technology Research and Development Center, Amagasaki-shi, Hyogo, Japan  
e-mail: [fujimoto.yasuhisa@db.MitsubishiElectric.co.jp](mailto:fujimoto.yasuhisa@db.MitsubishiElectric.co.jp)

This research aims to identify the coefficient of thermal expansion of dissimilar materials from displacement distribution. Here, the dissimilar materials simulate a mounting structure of soldered joints and the laminates of electric mounting boards. Displacement distribution measured using digital image correlation (DIC) [6] is used as the input and the virtual fields method is used as an inverse analysis method. Results of a uniform thermal loading test show the effectiveness of the proposed method.

## Methods

### *Basic Principle of the Virtual Fields Method*

VFM is used for identification of the coefficient of thermal expansion of a test specimen. This method is based on the principle of virtual work. When an arbitrary virtual displacement is given to an object in equilibrium state, external virtual work and internal virtual work are equal. The principle of virtual work is expressed as

$$\int_{\Omega} \sigma_{ij} \varepsilon_{ij}^* d\Omega = \int_{\Gamma} T_i u_i^* d\Gamma \quad (12.1)$$

In this equation,  $\sigma_{ij}$  is the stress component,  $\varepsilon_{ij}^*$  is the virtual strain component,  $T_i$  is the traction,  $u_i^*$  is the virtual displacement,  $\Omega$  is the analysis area and  $\Gamma$  is the boundary surface of  $\Omega$  that is subjected to external loading. The subscripts  $i$  and  $j$  indicate the  $x$  and  $y$  directions in the Cartesian coordinate system.

Considering an elastic body as a test specimen, the stress-strain relationship can be expressed as follows with the stiffness matrix.

$$\begin{Bmatrix} \sigma_1 \\ \sigma_2 \\ \sigma_6 \end{Bmatrix} = \begin{bmatrix} C_{11} & C_{12} & 0 \\ C_{12} & C_{22} & 0 \\ 0 & 0 & C_{66} \end{bmatrix} \begin{Bmatrix} \varepsilon_1 \\ \varepsilon_2 \\ \varepsilon_6 \end{Bmatrix} \quad (12.2)$$

where  $\sigma_1$  and  $\sigma_2$  are the normal stresses,  $\sigma_6$  is the shear stress,  $\varepsilon_1$  and  $\varepsilon_2$  the normal strains, and  $\varepsilon_6$  is the shear strain, respectively. In Eq. (12.2),  $C_{11}$ ,  $C_{12}$ ,  $C_{22}$  and  $C_{66}$  are the elastic constants, and relate the elastic modulus and Poisson's ratio. The following equation is obtained from Eqs. (12.1) and (12.2).

$$C_{11} \int_{\Omega} \left( \varepsilon_1 \varepsilon_1^* + \varepsilon_2 \varepsilon_2^* + \frac{1}{2} \varepsilon_6 \varepsilon_6^* \right) d\Omega + C_{12} \int_{\Omega} \left( \varepsilon_2 \varepsilon_1^* + \varepsilon_1 \varepsilon_2^* - \frac{1}{2} \varepsilon_6 \varepsilon_6^* \right) d\Omega = \int_{\Gamma} (T_1 u_1^* + T_2 u_2^*) d\Gamma \quad (12.3)$$

In Eq. (12.3),  $\varepsilon_1$ ,  $\varepsilon_2$  and  $\varepsilon_6$  are the strain components in the target object and can be obtained by differentiating the measured displacement. Also,  $u_1^*$  and  $u_2^*$  are the virtual displacement components, and  $\varepsilon_1^*$ ,  $\varepsilon_2^*$  and  $\varepsilon_6^*$  are the virtual strain components that can be obtained by differentiating the virtual displacements. Unknown parameters  $C_{11}$  and  $C_{12}$  can be obtained by substituting two kinds of virtual displacement into Eq. (12.3) and solving it.

### *Identification of the Coefficient of Thermal Expansion*

In order to apply the virtual fields method to the identification of the coefficient of thermal expansion, considering the thermal load. Since the test specimen is not bounded in this test, it is assumed that  $T_i = 0$ , and Eq. (12.1) can be expressed as

$$\int_{\Omega} \sigma_{ij} \varepsilon_{ij}^* d\Omega = 0 \quad (12.4)$$

As the temperature changes, the size and shape of the object change and displacement, strain and stress are generated. The generated displacement, strain and stress due to temperature change, are referred to as thermal displacement, thermal strain and thermal stress, respectively. Since the total strain is the sum of the thermal strain and the elastic strain, it is expressed by the following equation.

$$\varepsilon^{\text{all}} = \varepsilon + \varepsilon^{\text{th}} \quad (12.5)$$

where  $\varepsilon^{\text{all}}$  is the total strain,  $\varepsilon$  is the elastic strain,  $\varepsilon^{\text{th}}$  is the thermal strain. The following equation is obtained from Eqs. (12.2) and (12.5). At this time, since deformation due to heat is not related to shear stress and shear strain,  $\sigma_6$  and  $\varepsilon_6$  do not change.

$$\begin{Bmatrix} \sigma_1 \\ \sigma_2 \\ \sigma_6 \end{Bmatrix} = \begin{bmatrix} C_{11} & C_{12} & 0 \\ C_{12} & C_{22} & 0 \\ 0 & 0 & C_{66} \end{bmatrix} \begin{Bmatrix} \varepsilon_1 - \varepsilon_x^{\text{th}} \\ \varepsilon_2 - \varepsilon_y^{\text{th}} \\ \varepsilon_6 \end{Bmatrix} \quad (12.6)$$

where  $\varepsilon_x^{\text{th}}$  and  $\varepsilon_y^{\text{th}}$  can be expressed as  $\alpha T$ .  $\alpha$  is the coefficient of thermal expansion and  $T$  is the temperature change. The following equation is obtained from Eqs. (12.3) and (12.6).

$$C_{11} \int_{\Omega} \left( \varepsilon_1 \varepsilon_1^* + \varepsilon_2 \varepsilon_2^* + \frac{1}{2} \varepsilon_6 \varepsilon_6^* \right) d\Omega + C_{12} \int_{\Omega} \left( \varepsilon_2 \varepsilon_1^* + \varepsilon_1 \varepsilon_2^* - \frac{1}{2} \varepsilon_6 \varepsilon_6^* \right) d\Omega = \alpha T \int_{\Omega} (C_{11} + C_{12}) (\varepsilon_1^* + \varepsilon_2^*) d\Omega \quad (12.7)$$

The inverse analysis can be carried out by giving virtual displacements corresponding to the number of materials when only the coefficient of thermal expansion is unknown parameter.

In the case of identifying the material properties of the dissimilar materials composed of three different metals, the following equation can be obtained from the Eq. (12.7) when the three kinds of materials are A, B and C, respectively.

$$\begin{aligned} & C_{11}^A \int_{\Omega^A} \left( \varepsilon_1^A \varepsilon_1^* + \varepsilon_2^A \varepsilon_2^* + \frac{1}{2} \varepsilon_6^A \varepsilon_6^* \right) d\Omega + C_{12}^A \int_{\Omega^A} \left( \varepsilon_2^A \varepsilon_1^* + \varepsilon_1^A \varepsilon_2^* - \frac{1}{2} \varepsilon_6^A \varepsilon_6^* \right) d\Omega \\ & + C_{11}^B \int_{\Omega^B} \left( \varepsilon_1^B \varepsilon_1^* + \varepsilon_2^B \varepsilon_2^* + \frac{1}{2} \varepsilon_6^B \varepsilon_6^* \right) d\Omega + C_{12}^B \int_{\Omega^B} \left( \varepsilon_2^B \varepsilon_1^* + \varepsilon_1^B \varepsilon_2^* - \frac{1}{2} \varepsilon_6^B \varepsilon_6^* \right) d\Omega \\ & + C_{11}^C \int_{\Omega^C} \left( \varepsilon_1^C \varepsilon_1^* + \varepsilon_2^C \varepsilon_2^* + \frac{1}{2} \varepsilon_6^C \varepsilon_6^* \right) d\Omega + C_{12}^C \int_{\Omega^C} \left( \varepsilon_2^C \varepsilon_1^* + \varepsilon_1^C \varepsilon_2^* - \frac{1}{2} \varepsilon_6^C \varepsilon_6^* \right) d\Omega \\ & = C_{11}^A \alpha^A T^A \int_{\Omega^A} (\varepsilon_1^* + \varepsilon_2^*) d\Omega + C_{12}^A \alpha^A T^A \int_{\Omega^A} (\varepsilon_1^* + \varepsilon_2^*) d\Omega \\ & + C_{11}^B \alpha^B T^B \int_{\Omega^B} (\varepsilon_1^* + \varepsilon_2^*) d\Omega + C_{12}^B \alpha^B T^B \int_{\Omega^B} (\varepsilon_1^* + \varepsilon_2^*) d\Omega \\ & + C_{11}^C \alpha^C T^C \int_{\Omega^C} (\varepsilon_1^* + \varepsilon_2^*) d\Omega + C_{12}^C \alpha^C T^C \int_{\Omega^C} (\varepsilon_1^* + \varepsilon_2^*) d\Omega \end{aligned} \quad (12.8)$$

Following equation is obtained by giving three types of virtual displacements for unknowns.

$$\begin{pmatrix} P^{(1)} \\ P^{(2)} \\ P^{(3)} \end{pmatrix} = T \begin{bmatrix} Q^{A(1)} & Q^{B(1)} & Q^{C(1)} \\ Q^{A(2)} & Q^{B(2)} & Q^{C(2)} \\ Q^{A(3)} & Q^{B(3)} & Q^{C(3)} \end{bmatrix} \begin{pmatrix} \alpha^A \\ \alpha^B \\ \alpha^C \end{pmatrix} \quad (12.9)$$

where

$$\begin{aligned} P^{(1)} &= C_{11}^A \int_{\Omega^A} \left( \varepsilon_1^A \varepsilon_1^{*(1)} + \varepsilon_2^A \varepsilon_2^{*(1)} + \frac{1}{2} \varepsilon_6^A \varepsilon_6^{*(1)} \right) d\Omega + C_{12}^A \int_{\Omega^A} \left( \varepsilon_2^A \varepsilon_1^{*(1)} + \varepsilon_1^A \varepsilon_2^{*(1)} - \frac{1}{2} \varepsilon_6^A \varepsilon_6^{*(1)} \right) d\Omega \\ & + C_{11}^B \int_{\Omega^B} \left( \varepsilon_1^B \varepsilon_1^{*(1)} + \varepsilon_2^B \varepsilon_2^{*(1)} + \frac{1}{2} \varepsilon_6^B \varepsilon_6^{*(1)} \right) d\Omega + C_{12}^B \int_{\Omega^B} \left( \varepsilon_2^B \varepsilon_1^{*(1)} + \varepsilon_1^B \varepsilon_2^{*(1)} - \frac{1}{2} \varepsilon_6^B \varepsilon_6^{*(1)} \right) d\Omega \\ & + C_{11}^C \int_{\Omega^C} \left( \varepsilon_1^C \varepsilon_1^{*(1)} + \varepsilon_2^C \varepsilon_2^{*(1)} + \frac{1}{2} \varepsilon_6^C \varepsilon_6^{*(1)} \right) d\Omega + C_{12}^C \int_{\Omega^C} \left( \varepsilon_2^C \varepsilon_1^{*(1)} + \varepsilon_1^C \varepsilon_2^{*(1)} - \frac{1}{2} \varepsilon_6^C \varepsilon_6^{*(1)} \right) d\Omega \\ Q^{A(1)} &= C_{11}^A \int_{\Omega^A} (\varepsilon_1^* + \varepsilon_2^*) d\Omega + C_{12}^A \int_{\Omega^A} (\varepsilon_1^* + \varepsilon_2^*) d\Omega \end{aligned} \quad (12.10)$$

The superscript of  $P$  and  $Q$  describes the index of virtual displacement. Equation (12.9) can be expressed as following equation.

$$\mathbf{P} = \mathbf{Q}\mathbf{R} \quad (12.11)$$

Equation (12.11) is simultaneous equations relating to unknown parameters  $\alpha^A$ ,  $\alpha^B$  and  $\alpha^C$ . Therefore, the coefficient of thermal expansion can be obtained from multiplying the left side of both sides of equation by the inverse matrix  $\mathbf{Q}^{-1}$ .

## Experiment

### Specimen

To verify the effectiveness of the proposed method, a thermal load test is carried out with dissimilar materials composed three kinds of metal with the coefficient of thermal expansion mismatch. Figure 12.1 shows the dimensions and shape of an example test specimen schematically. Silver solder is used for adhesion and the joining method is torch brazing. For the specimen, heterojointed body consisting of a low coefficient of thermal expansion and a high coefficient of thermal expansion simulating the substrate structure is used. Most of the laminate has three layers or more and a structure including an intermediate layer. Therefore, to observe the influence by the dimension of the width, four kinds of test specimen with different widths of the intermediate layer are used. The size of the test specimen is  $10 \times 10 \times 3$  mm at both ends, and the intermediate layer has 4 types of length and thickness of  $10 \times 3$  mm, width of 2, 4, 7 and 10 mm. Combination of the test piece used for the heat load test is C2801-C1020-SUS430. Table 12.1 shows the material properties of each material.

### Experimental and Analysis Procedure

A test specimen is placed in a heat spreader in a thermostatic chamber. A CCD camera is placed above the thermostat to capture the deformation behavior of the test specimen. The temperature in the chamber can be controlled in the increments of  $1^\circ\text{C}$ . The test specimen is heated from the room temperature ( $25^\circ\text{C}$ ) to  $75^\circ\text{C}$  ( $\Delta 50^\circ\text{C}$ ),  $100^\circ\text{C}$  ( $\Delta 75^\circ\text{C}$ ),  $125^\circ\text{C}$  ( $\Delta 100^\circ\text{C}$ ),  $150^\circ\text{C}$  ( $\Delta 125^\circ\text{C}$ ) and  $175^\circ\text{C}$  ( $\Delta 150^\circ\text{C}$ ) and a uniform heat load is applied to the test piece. The displacement distribution of the surface of the test specimen is measured from the photographed images. DIC is used for the displacement measurement. DIC is performed from images obtained before and after the uniform thermal load test. A telecentric lens is attached to a CCD camera whose resolution is  $2048 \times 2048$  pixels and its bit depth is 8 bits. The subset size for analysis is  $31 \times 31$  pixels. A test specimen is coated with a random pattern of the surface with a black and white lacquer spray.

Figure 12.2 shows the mesh models used for inverse analysis in this experiment, which are constructed using 8 node isoparametric elements. A similar analysis is carried out using mesh model which is 75 elements model. The displacement data is allocated to each node point of the mesh model and the inverse analysis is performed. The integral calculation included in Eq. (12.7) is executed by piecewise virtual fields [7, 8] with the mesh model [9].

Fig. 12.1 Test specimen

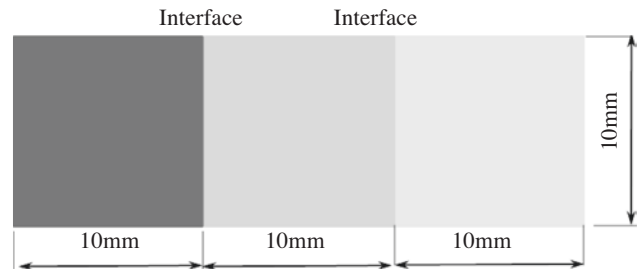
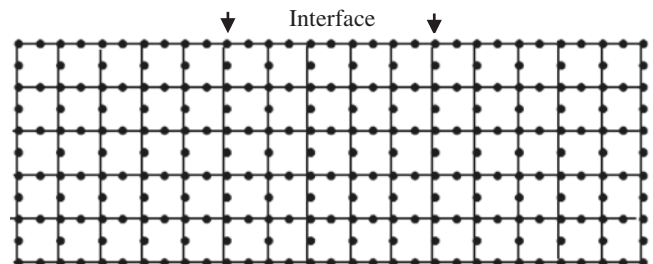


Table 12.1 Material properties

Material	Elastic modulus (GPa)	Poisson's ratio	Coefficient of thermal expansion (ppm/ $^\circ\text{C}$ )
C2801 (brass)	103	0.35	19.5
C1020 (copper)	118	0.33	17.4
SUS430 (stainless steel)	206	0.30	10.3

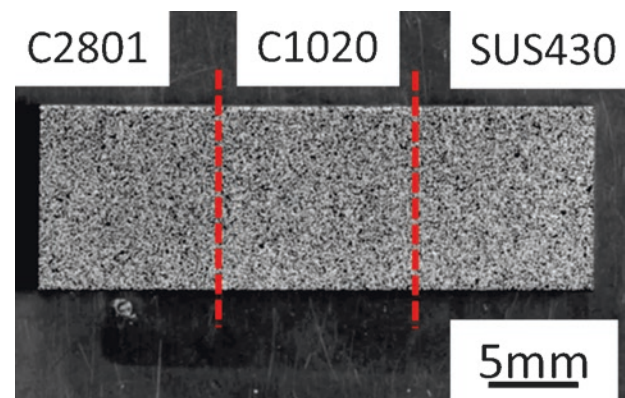
Fig. 12.2 Mesh model  
(nodes: 266, elements:75)



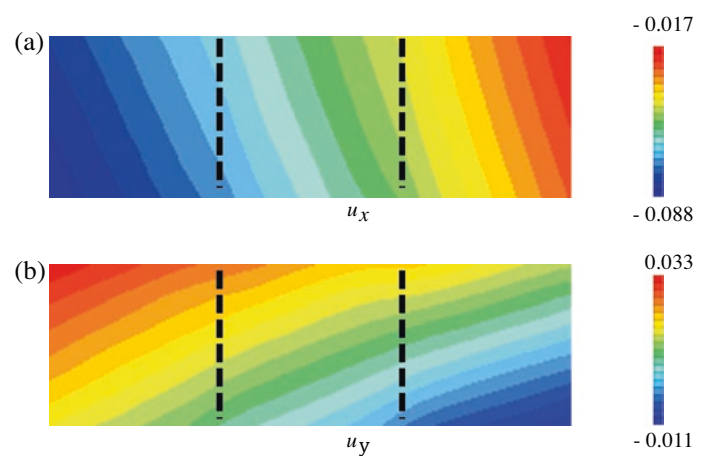
## Results

Figure 12.3 shows the surface image of the test specimen at the reference temperature (25 °C) before thermal loading. The red dash line indicates the interface. Displacement distribution data are obtained from DIC, taking the image of specimens before uniform thermal loading as the reference image. A displacement fields measured by DIC for a uniform thermal loading test are shown in Fig. 12.4. The results of displacement distribution is not uniform and increase as the temperature increase, and results show that  $u_x$  and  $u_y$  of the brass on the left side of the test specimen are large, respectively. Each of the three virtual displacements is prepared by performing a finite element analysis of the mesh model shown in Fig. 12.2. Using the proposed method the coefficient of the thermal expansion is identified from the input value of the displacement distribution. The identified results for the coefficient of thermal expansion are presented in Table 12.2. The results of each material are close to the reference value. Moreover, even if the width of C1020 (Copper) which is the intermediate layer changed, results are close to the reference. Influence due to the difference in width of the intermediate layer of the test specimen is not observed.

**Fig. 12.3** Image of test specimen



**Fig. 12.4** Displacement distribution ( $\Delta T = 150$  °C, unit: mm)



**Table 12.2** Inverse analysis result ( $\Delta T = 150$  °C)

	Coefficient of thermal expansion (ppm/°C)		
	C2801 (brass)	C1020 (copper)	SUS430 (stainless steel)
Reference	19.5	17.4	10.3
2 mm	19.7	17.6	10.3
4 mm	19.8	17.6	10.4
7 mm	19.7	17.6	10.5
10 mm	19.7	17.2	10.4

## Conclusions

This study proposes a method for identifying the coefficient of thermal expansion of dissimilar materials composed of three kinds of materials simulating a substrate. A uniform thermal load test is carried out to verify the effectiveness of the proposed method. The identification result is closed to reference value. In addition, the difference in width of intermediate layer of the test specimen does not affect.

## References

1. A. Khalilollahi, W. Russell, L.O. Onipede, *Thermal Reliability Design and Optimization for Multilayer Composite Electronic Boards* (ASME, International Mechanical Engineering Congress and Exposition, New York, 2005), pp. 845–851
2. M. Grédiac, F. Pierron, A. Vautrin, The iosipescu in-plane shear test applied to composites: a new approach based on displacement field processing. *Compos. Sci. Technol.* **51**(3), 409–417 (1994)
3. M.A. Sutton, J.H. Yan, S. Avril, F. Pierron, S.M. Adeb, Identification of heterogeneous constitutive parameters in a welded specimen: uniform stress and virtual fields methods for material property estimation. *Exp. Mech.* **48**(4), 451–464 (2008)
4. M. Grédiac, F. Pierron, Identifying constitutive parameters from heterogeneous strain fields using the virtual fields method. *Proc. IUTAM* **4**, 48–53 (2012)
5. Y. Sato, S. Arikawa, S. Yoneyama, Identification of elastic material characteristics of dissimilar materials by virtual fields method (in Japanese). *J. JSEM* **14**, 250–256 (2014)
6. S. Yoneyama, Basic principle of digital image correlation for inplane displacement and strain measurement. *Adv. Compos. Mater.* **25**, 105–123 (2015)
7. M. Grédiac, F. Pierron, S. Avril, E. Toussaint, The virtual fields method for extracting constitutive parameters from full-field measurements: a review. *Strain* **42**, 233–253 (2006)
8. S. Yoneyama, P.G. Ifju, S.E. Rohde, Identifying through-thickness material properties of carbon-fiber-reinforced plastics using the virtual fields method combined with moiré interferometry. *Adv. Compos. Mater.* **27**, 1–17 (2018)
9. D.J. Segalman, D.B. Woyak, R.E. Rowlands, Smooth spline-like finite element differentiation of full-field experimental data over arbitrary geometry. *Exp. Mech.* **19**, 429–437 (1979)